Comparing and Developing PID and Sliding Mode Controllers for Quadrotor

Ceren Cömert and Coşku Kasnakoğlu
Electrical and Electronics Engineering, TOBB University of Economics and Technology, Ankara, Turkey
Email: {ccomert, kasnakoglu}@etu.edu.tr

***Abstract*—This paper provides information about controller design for quadrotors which became an essential research topic. Sliding mode control (SMC) provides better solutions to problems that can be caused by model discrepancies. Firstly, sliding mode controllers are designed for altitude, roll, pitch and yaw angle controls. One common problem of sliding mode control, chattering is eliminated. Then, proportional integral derivative (PID) controller is developed in order to compare and discuss simulation results. Coefficients are tuned by iteration method in both PID and SMC designs. It can be interpreted that the controllers of both designs are capable of tracking the desired values.**

***Index Terms*—unmanned aerial vehicle, quadcopter, sliding mode control, quadrotor, proportional integral derivative, nonlinear control**

I. Introduction

Unmanned aerial vehicles became an essential research topic due to their vast application areas. Search and rescue, transportation, fire monitoring, military and defense, crop spraying and are some of the areas that they can be used. Because of their maneuverability, quadrotor are often used for controller designs [1]-[4].

Quadrotors are unmanned aerial vehicles whose four rotors can be controlled separately. This situation gives the capability to move rotational and translational in three dimensional space called six degrees of freedom (6DOF).

Fig. 1 demonstrates quadrotors' movements and angles which occur between earth and body fixed frames [5]-[9].

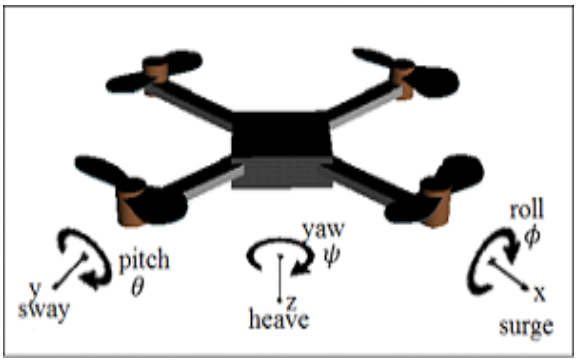

Figure 1. Six degrees of freedom.

Manuscript received January 20, 2017; revised April 25, 2017.

It is possible to make transition between earth frame and body frame.

Equation (1) through "(4)" show the transformation between two referential frames [10], [11].

$$\begin{bmatrix} \dot{x} \\ \dot{y} \\ \dot{z} \end{bmatrix} = R(\psi)R(\theta)R(\phi) * \begin{bmatrix} u \\ v \\ w \end{bmatrix} \tag{1}$$

$$R(\psi) = \begin{bmatrix} \cos(\psi) & -\sin(\psi) & 0 \\ \sin(\psi) & \cos(\psi) & 0 \\ 0 & 0 & 1 \end{bmatrix} \tag{2}$$

$$R(\theta) = \begin{bmatrix} \cos(\theta) & 0 & \sin(\theta) \\ 0 & 1 & 0 \\ -\sin(\theta) & 0 & \cos(\theta) \end{bmatrix} \tag{3}$$

$$R(\phi) = \begin{bmatrix} 1 & 0 & 0 \\ 0 & \cos(\phi) & -\sin(\phi) \\ 0 & \sin(\phi) & \cos(\phi) \end{bmatrix} \tag{4}$$

A. Force and Torgue Formulas

Equation (5) shows inertia matrix of the quadrotor which will be used for attitude controller design. Inertia matrix is used to determine the torque needed for a desired angular acceleration about a rotational axis [12].

$$J = \begin{bmatrix} Jx & 0 & 0 \\ 0 & Jy & 0 \\ 0 & 0 & Jz \end{bmatrix} \tag{5}$$

Using Newton-Euler law, the force and torque formulas can be defined in ''(6)" and ''(7)".

In these equations F represents force, τ represents torque and m represents mass. u, v and w are velocities, while p, q, and r stand for angular rates[5], [13], [14]

$$\begin{bmatrix} F_x \\ F_y \\ F_z \end{bmatrix} = m \begin{bmatrix} \dot{u} \\ \dot{v} \\ \dot{w} \end{bmatrix} + m \begin{bmatrix} qw - rv \\ ru - pw \\ pv - qu \end{bmatrix} \tag{6}$$

$$\begin{bmatrix} \tau_x \\ \tau_y \\ \tau_z \end{bmatrix} = \begin{bmatrix} \dot{p} J_x \\ \dot{q} J_y \\ \dot{r} J_z \end{bmatrix} + \begin{bmatrix} qr(J_z - J_y) \\ pr(J_x - J_z) \\ pq(J_y - J_x) \end{bmatrix} \tag{7}$$

B. Transformation Matrix

Equation (8) and ''(9)" show the transformation matrix [15], [16].

$$\begin{bmatrix} \dot{\phi} \\ \dot{\theta} \\ \dot{\psi} \end{bmatrix} = \begin{bmatrix} 1 & \sin(\phi)\tan(\theta) & \cos(\phi)\tan(\theta) \\ 0 & \cos(\phi) & -\sin(\phi) \\ 0 & \sin(\phi)/\cos(\theta) & \cos(\phi)/cos(\theta) \end{bmatrix} \begin{bmatrix} p \\ q \\ r \end{bmatrix} \tag{8}$$

doi: 10.18178/ijmerr.6.3.194-199

$$\begin{bmatrix} p \\ q \\ r \end{bmatrix} = \begin{bmatrix} 1 & 0 & -\sin(\theta) \\ 0 & \cos(\phi) & \cos(\theta)\sin(\phi) \\ 0 & -\sin(\phi) & \cos(\theta)\cos(\phi) \end{bmatrix} * \begin{bmatrix} \dot{\phi} \\ \dot{\theta} \\ \dot{\psi} \end{bmatrix} \quad (9)$$

C. Types of Configurarion

Cross-configuration and plus-configuration are two common types of configuration for quadcopters. For plus configuration, two motors oppose each other in order to control the roll rotation while the other two control the pitch rotation. To illustrate, changing the balance of the speed of the rotors on the roll axis creates roll movement [17], [18].

On the other hand, all the four motors are required for both roll and pitch rotation for cross configuration [19]. In order to control altitude and yaw movement all four motors are used for both configurations.

Plus configuration is considered more acrobatic structure when compared the cross configuration. Cross configuration is more stable [20], [21]. Cross configuration is usually preferred if quadcopter consist a camera [22].

In this paper plus configuration is considered. Fig. 2 shows two common types of configurations for quadcopters.

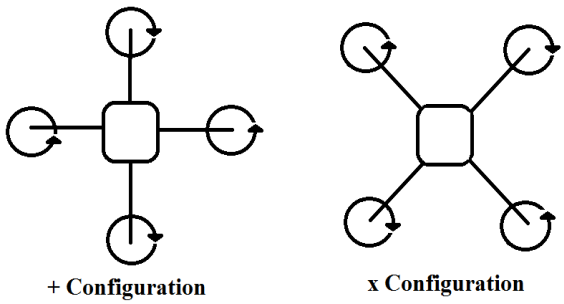

Figure 2. Quadrotor configurations

II. Sliding Mode Control

Disturbances, dynamics, plant parameters causes discrepancies between the actual system and mathematical model. To solve this problem, robust control methods are developed. Sliding mode controller (SMC) is the one of the robust control design approaches [23].

In sliding mode controller design, the main purpose is to keep plant at the desired sliding surface. If the system in "(10)" is considered

$$x^{(n)} = f(x) + b(x)u \quad (10)$$

where x is the output, u is the controller input and f(x) is the function whose boundaries are known and b(x) is the function whose boundaries and sign are known, sliding surface is defined in "(11)" where λ is positive constant [24].

$$s = (d/dt + \lambda)^{n-1}\, e \quad (11)$$

$$e = x - x_d \quad (12)$$

For a second order system sliding surface is defined in "(13)". [24].

$$s = \dot{e} + \lambda e \quad (13)$$

$$\dot{s} = \ddot{e} + \lambda\dot{e} = \ddot{x} - \ddot{x}_d = f(x) + u - \ddot{x}_d + \lambda e \quad (14)$$

Sliding condition is defined in ''(15)''. If a controller is designed to achieve $\dot{s}$ zero and f(x) predicted as $\hat{f}(x)$ then the new controller input is given in "(16)". [24], [25].

$$\frac{1}{2}\frac{d}{dt}(s^2) \leq -\eta|s| \quad (15)$$

$$u = -\hat{f}(x) + \ddot{x}_d - \lambda\dot{e} - k\,\mathrm{sign}(s) \quad (16)$$

Equation (17) defines sign function.

$$\mathrm{sign}(s) = \begin{cases} -1 & s < 0 \\ 1 & s > 0 \end{cases} \quad (17)$$

Derivative of the sliding surface is obtained as in ''(18)''[24], [26], [27].

$$\dot{s} = -k_1 s - k_2\,\mathrm{sign}(s) \quad (18)$$

A. Altitude Controller

Equation (19) represent quadrotor dynamics for altitude. By equating "(14)" and "(18)" and substituting $\ddot{z}$ from "(19)", the input for the altitude controller is calculated as in "(20)" [24], [28], [29].

$$\ddot{z} = g - U_1\cos(\phi)\cos(\theta)/m \quad (19)$$

$$U_1 = \frac{m}{\cos(\phi)\cos(\theta)} k_1 s + k_2\,\mathrm{sign}(s) + \lambda(\dot{z}_{ref} - \dot{z}) + g - \ddot{z}_{ref} \quad (20)$$

The MATLAB Simulink model designed for the altitude control, is shown in Fig. 3.

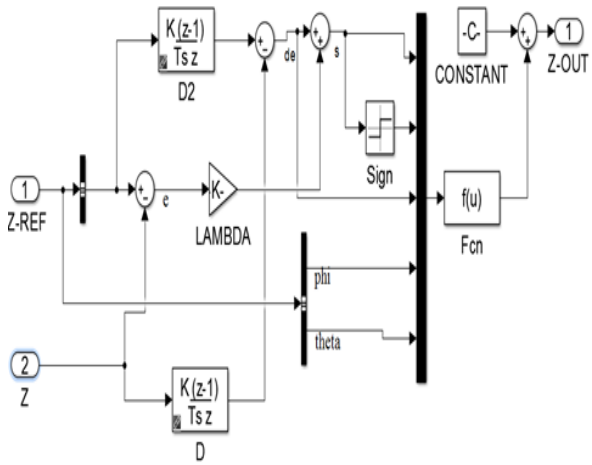

Figure 3. SMC altitude controller Simulink model

Table I shows sliding mode coefficients for altitude control.

TABLE I. SMC Coeeficients for Altitude Control

Name	Value
k_1	1
k_2	12
λ	20

B. Attitude Controller

Dynamic model equations for roll, pitch and yaw are given in the "(21)" through "(23)" respectively. Controller inputs are obtained by substituting $\ddot{\phi}$, $\ddot{\theta}$ and $\ddot{\psi}$ from these three are equations.

$$\ddot{\phi} = \frac{d}{Jx} U_2 - \frac{Jm}{Jx}\dot{\theta}\Omega + \frac{Jy-Jz}{Jx}\dot{\theta}\dot{\psi} \tag{21}$$

$$\ddot{\theta} = \frac{d}{Jy} U_3 - \frac{Jm}{Jy}\dot{\phi}\Omega + \frac{Jz-Jx}{Jy}\dot{\phi}\dot{\psi} \tag{22}$$

$$\ddot{\psi} = \frac{d}{Jz} U_4 + \frac{Jx-Jy}{Jz}\dot{\phi}\dot{\theta} \tag{23}$$

Sliding mode controller inputs for roll angle (phi), pitch angle (theta) and yaw angle (psi) are given in the "(24)","(25)" and "(26)" respectively [28], [30], [31].

$$U_2 = \frac{Jx}{L}[k_1 s + k_2 \mathrm{sign}(s) + \lambda(\dot{\phi}_{ref} - \dot{\phi}) + \ddot{\phi}_{ref} + \frac{Jm}{Jx}\dot{\theta}\Omega - \frac{Jy-Jz}{Jz}\dot{\theta}\dot{\psi}] \tag{24}$$

$$U_3 = \frac{Jy}{L}[k_1 s + k_2 \mathrm{sign}(s) + \lambda(\dot{\theta}_{ref} - \dot{\theta}) + \ddot{\theta}_{ref} + \frac{Jm}{Jy}\dot{\phi}\Omega - \frac{Jz-Jx}{Jy}\dot{\phi}\dot{\psi}] \tag{25}$$

$$U_4 = \frac{Jz}{L}[k_1 s + k_2 \mathrm{sign}(s) + \lambda(\dot{\psi}_{ref} - \dot{\psi}) + \ddot{\psi}_{ref} - \frac{Jx-Jy}{Jz}\dot{\phi}\dot{\theta}] \tag{26}$$

C. Chattering Reduction

Chattering problem often occurs in sliding mode designs. One reason for chattering to occur is fast dynamics which are neglected by model causing fast switching of sliding mode controllers [32], [33]. Chattering effect is demonstrated in Fig. 4.

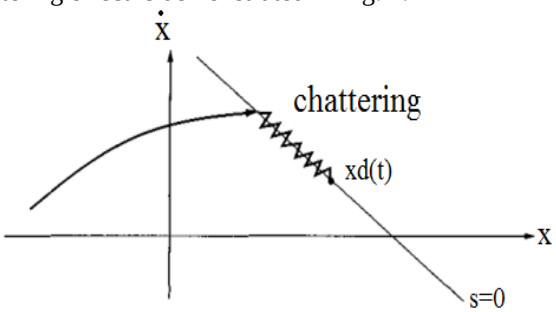

Figure 4. Chattering effect

A common way to solve this problem is to introduce a boundary layer around the surface [34]. This method provides a smooth continuous approach to the discontinuous sign function by a continuous function [25]. The most commonly used functions for chattering elimination are saturation [34], [35] and sigmoid [23] functions. Saturation and sigmoid functions are given ''(27)'' and ''(28)'' respectively.

$$sat\left(\frac{s}{\varphi}\right) = \begin{cases} \frac{s}{\varphi}, & \frac{s}{\varphi} \le 1 \\ sign(\frac{s}{\varphi}), & \frac{s}{\varphi} > 1 \end{cases} \tag{27}$$

$$\mathrm{sigmoid}(s) = \frac{s}{|s|+\varepsilon} \tag{28}$$

ε is positive constant and φ represents boundary stickness.

In order to reduce chattering sign function in the altitude control model is changed with the sigmoid function, while the ones in the attitude control models (phi, theta and psi models) are changed with the saturation function.

Because of overshoot increase in phi and theta, an integrator is added to the sliding surface as illustrated in the"(29)" and "(30)" for the roll and pitch angle control [24], [35].

$$s = (d/dt + \lambda)^{n-1} \int e\, dr \tag{29}$$

$$s = \dot{e} + 2\lambda e + \lambda^2 \int e\, dr \tag{30}$$

Simulink model used for roll, pitch and angle control is shown in Fig. 5.

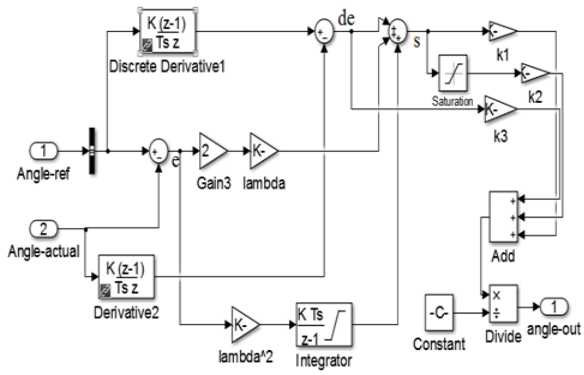

Figure 5. SMC roll and pitch controller Simulink model.

Table II demonstrates sliding mode coefficients for attitude control after chattering effect is eliminated. Coefficients for altitude sliding mode control remains the same.

TABLE II. SMC COEFFICIENTS FOR ATTITUDE CONTROL

Name	Angle		
	Roll	Pitch	Yaw
k_1	6	6	0.1
k_2	18.5	18.6	90
λ	0.27	0.27	2.5

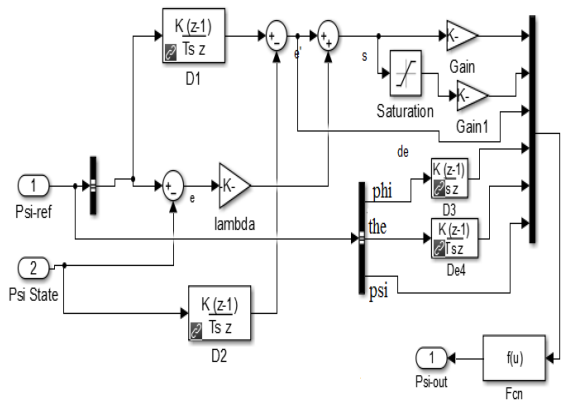

Figure 6. SMC yaw control simulink model

Simulink model used for yaw angle control is shown in Fig. 6.

III. PID Control

A. Altitude Control

Equation (29) represents PID altitude controller input.

$$U_1 = K_p(z_{ref}-z) + K_d(\dot{z}_{ref} - \dot{z}) + K_i\int(z_{ref} - z) \quad (29)$$

MATLAB Simulink model designed for the altitude control is shown in Fig. 7.

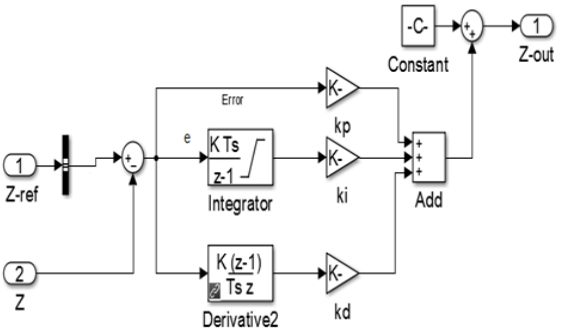

Figure 7. PID altitude controller Simulink model.

Table III demonstrates PID coefficients for altitude control.

TABLE III. PID Coeeficients for Altitude Control

Name	Value
Kp	2.6
Ki	0.5
Kd	3.7

Fig. 8 shows simulation results for altitude for both C and PID controllers.

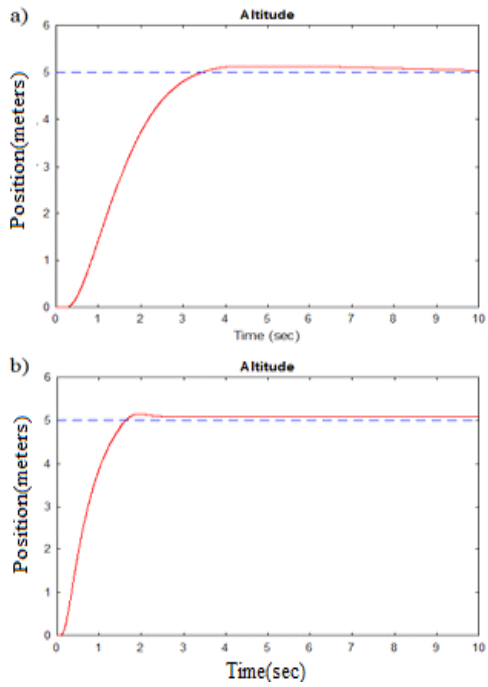

Figure 8. Simulation results for altitude model a) PID, b) SMC

B. Attitude Controller

The proportional-integral-derivative controller inputs for roll angle (ϕ), pitch angle (θ) and yaw angle (ψ) are given in the "(30)" through "(32)" [36].

$$U_2 = K_p(\phi_{ref} - \phi) + K_d(\dot{\phi}_{ref} - \dot{\phi}) + K_i\int(\phi_{ref} - \phi) \quad (30)$$

$$U_3 = K_p(\theta_{ref} - \theta) + K_d(\dot{\theta}_{ref} - \dot{\theta}) + K_i\int(\theta_{ref} - \theta) \quad (31)$$

$$U_4 = K_p(\psi_{ref} - \psi) + K_d(\dot{\psi}_{ref} - \dot{\psi}) + K_i\int(\psi_{ref} - \psi) \quad (32)$$

Simulink model designed for roll angle, pitch angle and yaw angle PID control is shown in Fig. 9.

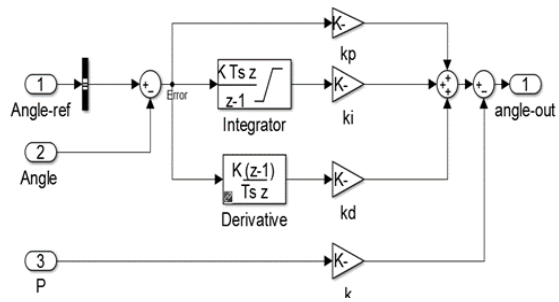

Figure 9. PID altitude controller Simulink model.

PID coefficients for attitude control are given in the Table IV.

TABLE IV. PID Coefficients for Attitude Control

Name	Angle		
	Roll	Pitch	Yaw
Kp	3	3	6
Ki	0.1	0.1	0.8
Kd	0.1	0.1	0.6
K	1.2	1.2	5.4

IV. Simulation Results for Attitude

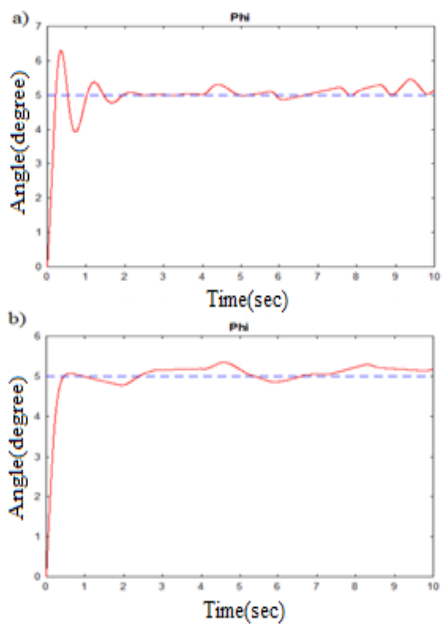

Figure 10. Simulation results for roll angle a) PID, b) SMC.

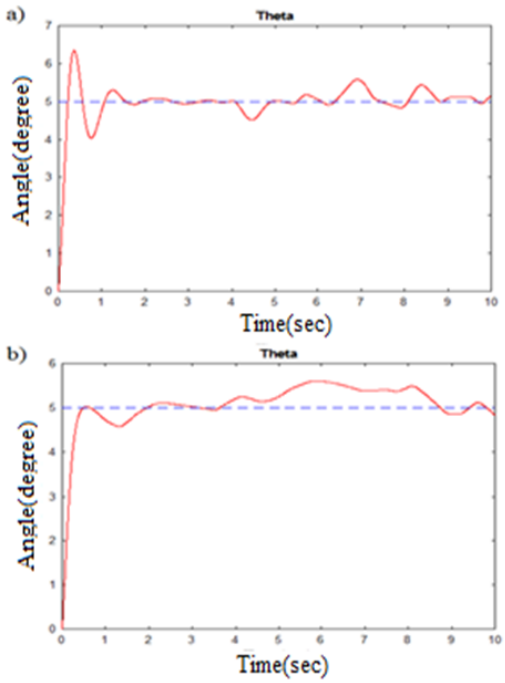

Figure 11. Simulation results for roll angle a) PID, b) SMC.

Fig. 10 through 13 shows simulation results which are obtained for both PID and sliding mode controllers.

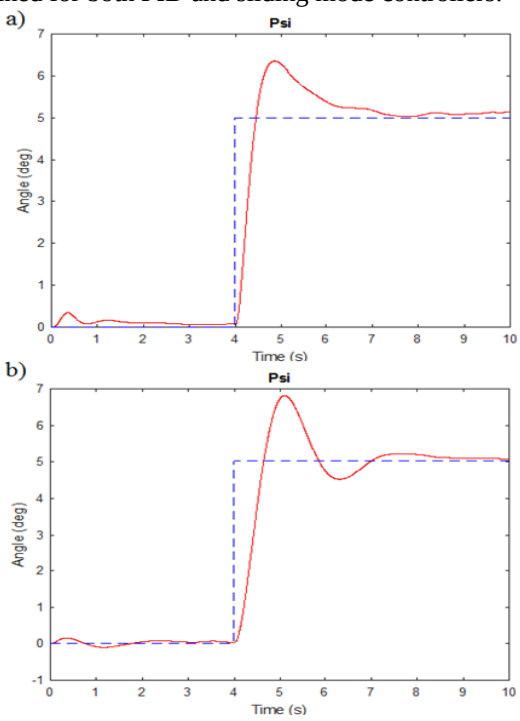

Figure 12. Simulation results for yaw angle a) PID, b) SMC.

V. Conclusion and Future Work

This paper represented both sliding mode controller and proportional integral derivative controller designs for a quadrotor. Firstly, both models are designed using MATLAB Simulink, then coefficients are tuned by iteration method.

After the coefficients are tuned for sliding mode controllers, chattering problem caused by fast dynamics and discontinuity is suppressed by using either saturation function or sigmoid function. After chattering is eliminated coefficients are readjusted and an integrator is added to the sliding surface for the roll and pitch angle controllers. The designed sliding mode controllers are capable of following altitude and attitude commands.

In order to reduce steady state error, angular rates (p, q and r) are used as a feedback in PID controller design. As a result, PID controllers are capable of tracking the desired values.

Simulation results reveals that the sliding mode controllers can track the desired values with faster response and less oscillation than the PID controllers.

Future research includes testing the theoretical simulation results on a quadcopter in order to obtain experimental results.

References

[1] A. Motaparthi, R. Katukam, "MAV for fire existinguiging a review," *International Journal of Engineering Innovation and Research*, vol. 3, pp. 297-299, 2014.

[2] K. Whitehead, C. H. Hugenholtz, S. Myshak, O. Brown, A. LeClair, *et al*., "Remote sensing of the environment with small unmanned aircraft systems, " *Journal of Unmanned Vehicle Systems*, vol. 3, pp. 86-102, 2014.

[3] H. Eisenbeiss, "A mini unmanned aerial vehicle system overview and image acqusition," in *Proc. International Workshop on Processing and Visualization Using High Resolution Imagery*, Thailand, 18-20 November, 2004.

[4] M. Wheeler, B. Schrick, W. Whitacre, M. Campbell, R. Rysdyk, and P. Wise, "Cooperative tracking of moving targets by a team of autonomous uavs," in *Proc. 25th Digital Avionics Systems Conference*, October 15-19, 2006.

[5] T. Jirinec, "Stabilization and control of unmanned quadcopter," M.S. thesis, Dept. of Cybernetics, Czech Technical Univ., Prague, Czech Pepublic, 2011.

[6] A. U. Batmaz, Ö. Elbir, and C. Kasnakoğlu, "Design of a quadrotor roll controller using system identification to improve empirical results," *International Journal of Materials, Mechanics and Manufacturing*, vol. 1, pp. 347-349, 2013.

[7] G. Malara, P. D. Spanos, and F. Arena, "Maximum roll angle estimatin of a ship in confused sea waves via a quasi-deterministic approach," *Probabilistic Engineering Mechanics*, vol. 35, pp. 75-81, 2014.

[8] D. Sandaruwan, N. Kodikara, C. Keppitiyagama, and R. Rosa, "A six degrees of freedom ship simulation system for maritime education," *The International Journal on Advances in ICT for Emerging Regions*, vol. 2, pp. 34-47, 2010

[9] M. B. Hurd, "Control of quadcopter aerial robot using optic flow sensing," M.S. thesis, University of Nevada, Reno, 2013.

[10] Ø. Magnussen and K. E. SkjØnhaug, "Modelling design and experimental study for quadcopter system construction," M.S. thesis, Dept. Eng, University of Adger, Norway, 2011.

[11] S. Stevanovic, J. Kasac, and J. Stepanic, "Robust tracking control of a quadrotor helicopter without velocity measurement," in *Proc. Annals of DAAAM for 2012 and Proceedings of the 23rd International DAAAM Symposium*, 2012, pp. 595-600.

[12] M. W. Mueller and R. D'Andrea, "Stability and control of a quadrocopter despite the complete loss of one, two or three propellers," in *Proc. IEEE International Conference on Robotics & Automation*, Hong Kong, China, June 2014, pp. 45-52.

[13] T. G. Carreria, "Quadcopter automatic landing and docking station," M.S thesis, Dept. Eng., Technico Lisboa, Lisboa, Portugal, 2013.

[14] S. Bouabdallah, "Design and control of quadrotors with application to autonomous flying," PhD thesis, Ecole Polytechnique Federale de Lausanne, Lausanne, 2007.

[15] C. Balas, "Modelling and linear control of quadrotor," M.S. thesis, Cranfield University, 2007.

[16] T. Luukkonen, "Modelling and control of a quadcopter, ındependet research project in applied mathematics," Aalto University, Espoo, 2011
[17] L. M. Argentim, W. C. Rezende, P. E. Santos, and R. A. Aguiar, 'PID, LQR and LQR-PID on a Quadcopter Platform," in *Proc. International Conference on Informatics, Electronics & Vision*, May 17-18, 2013.
[18] H. Bolandi, M Rezaei, R. Mohsenipour, H. Nemati, and S. M. Smailzadeh, "Attitude control of a quadrotor with optimized PID controller," *Intelligent Control and Automation*, vol. 4, pp. 335-342, 2013.
[19] H. L. Chan and K. T. Woo, "Design and control of small quadcopter system with motor closed loop speed control," *International Journal of Mechanical Engineering and Robotics Research*, vol. 4, pp. 287-292, October 2015.
[20] S. N. Ghazbi, Y. Aghli, M. Alimohammadi, and A. A. Akbari, "Quadrotors unmanned aerial vehicles a review," *International Journal on Smart Sensing and Intelligent Systems*, vol. 9, pp. 309-333, 2006.
[21] K. Agraval and P. Shirivastav, "Multirotors: A revolution in unmanned aerial vehicle," *International Journal of Science and Research*, vol. 4, pp. 1801-1804, 2015.
[22] R. Büchi, *Fascinating Quadcopter*, Norderstedt: Books on Demand, 2016.
[23] Y. Shtessel, C. Edwards, L. Fridman, and A. Levant, *Sliding Mode Control and Observation*, New York, Heidelberg, Dordrecht, London: Springer-Birkhauser, 2014, ch 1.
[24] J. E. Slotline and W. Li, *Applied Nonlinear Control*, Prentice Hall 1991, ch.7.
[25] F. Piltan, S. Rahmdel, S. Mehrara, and R. Bayat, "Sliding mode methodology vs. computed torque methodology using MATLAB/Simulink and their integration into graduate nonlinear control courses," *International Journal of Engineering*, vol. 6, no. 3, pp, 142-177, 2012.
[26] A. Sabanovic, L. M. Fridman, and S. Spurgeon, "Variable structure systems: From principles to implementation," *The Institution of Engineering and Technology*, 2004.
[27] L. Ding and S. Qui, "The research based on fuzzy sliding mode control for linear double inverted pendulum," *Advanced Materials Research*, vol. 926-930, pp. 1463-1467.
[28] H. Elkholy, "Dynamic modelling and control of a quadrotor using linear and nonlinear approaches," M.S. Thesis, The American University in Cario, Cario, Egypt, 2014.
[29] D. Kotarski, Z. Benic, and M. Krznar, "Control design for unmanned aerial vehciles with four rotors," *Interdisciplinary Description of Complex Systems*, vol. 14, no. 2, pp. 236-245, 2016.
[30] H. Bouadi and M. Tadjine, "Nonlinear observer design and sliding mode control of four rotors helicopter," *International Journal of Mechanical, Aerospace, Industrial, Mechatronic and Manufacturing Engineering*, vol. 1, pp. 329-334, 2007.
[31] S. Bouabdallah and R. Siegwart, "Backstepping and sliding mode techniques applied to am ındoor micro quadrotor," in *Proc. International Conference on Robotics and Automation*, Barcelona, Spain, 2005.
[32] V. Utkin, J. Guldner J. Shi, *Sliding Mode Control in Electromechanical Systems*, London, Philadelphia, Taylor & Francis, 1999, ch.8.
[33] J. Guldner and V. Utkin, "The chattering problem in sliding mode systems," in *Proc. 14th Internatiomal Sympsium on Mathematical Theory of Networks and Systems*, Perpignan, France.
[34] Y. Kim and G. Jeon, "Error reduction of sliding mode controller using sigmoid type nonlinear interpolation in the boundary layer," *IJCAS*, vol. 2, p. 4, 2004.
[35] Y. A. Ajmera and S. S. Sankeshwari, "Fuzzy fractional order sliding mode controller for DC motor," *International Journal of Advances in Engineering and Technology*, vol. 6, pp. 1876-1885, 2013.
[36] A. U. Batmaz, Ö. Elbir, and C. Kasnakoğlu, "Improving quadrotor 3-axes stabilization results using empirical results and system identification," in *Proc. 9th IEEE Asian Control Conference*, 2013.

Ceren Cömert is currently a master student at the Electrical & Electronics Engineering Department, TOBB University of Economics & Technology, Ankara, Turkey. She received the BSc degree in Electrical & Electronics Engineering in 2014 from the TOBB University of Economics & Technology, Ankara, Turkey. Unmanned aerial vehicles and control systems are her current research areas.

Coşku Kasnakoğlu obtained B.S. degrees from the Department of Electrical and Electronics Engineering and the Department of Computer Engineering at the Middle East Technical University (METU), Ankara, Turkey in 2000. He obtained his M.S. and Ph.D. degrees from the Department of Electrical and Computer Engineering at the Ohio State University (OSU), Columbus, Ohio, USA in 2003 and 2007. He is currently an associate professor in the Department of Electrical and Electronics Engineering at TOBB University of Economics and Technology in Ankara, Turkey. Dr. Kasnakoglu's current research interests include nonlinear control, flow control, unmanned air vehicles, dynamical modeling, adaptive control and linear parameter varying systems.